THE JOURNAL OF PHYSICAL CHEMISTRY LETTERS
A JOURNAL OF THE AMERICAN CHEMICAL SOCIETY

pubs.acs.org/JPCL

Letter

Guanosine Dianions Hydrated by One to Four Water Molecules

Samanta Makurat,[#] Qinqin Yuan,[#] Jacek Czub,[#] Lidia Chomicz-Mańka,[#] Wenjin Cao, Xue-Bin Wang,* and Janusz Rak*

Cite This: *J. Phys. Chem. Lett.* 2022, 13, 3230−3236

Read Online

ACCESS | Metrics & More | Article Recommendations | Supporting Information

ABSTRACT: Intermolecular interactions such as those present in molecule···water complexes may profoundly influence the physicochemical properties of molecules. Here, we carried out an experimental−computational study on doubly deprotonated guanosine monophosphate··· water clusters, $[dGMP - 2H]^{2-}{\cdot}nH_2O$ (n = 1−4), using a combination of negative anion photoelectron spectroscopy (NIPES) with molecular dynamics (MD) and quantum chemical (QM) calculations. Successive addition of water molecules to $[dGMP - 2H]^{2-}$ increases the experimental adiabatic detachment (ADE) and vertical detachment energy (VDE) by 0.5−0.1 eV, depending on the cluster size. In order to choose the representative conformations, we combined MD simulations with a clustering procedure to identify low energy geometries for which ADEs and VDEs were computed at the CAM-B3LYP/6-31++G(d,p) level. Our results demonstrate that the assumed approach leads to sound geometries and energetics of the studied microsolvates since the calculated ADEs and VDEs are in pretty good agreement with the experimental characteristics. The evolution of hydrogen bonding with cluster size indicates the possibility of the occurrence of proton transfer for clusters comprising a larger number of water molecules.

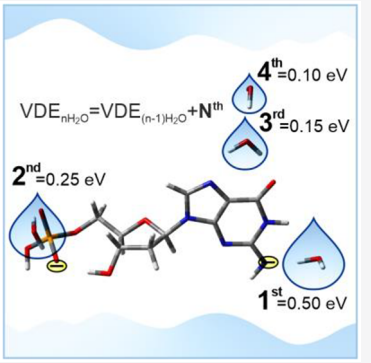

Radiation-induced DNA damage, such as strand breaks, mutations, photolesions, and transcription errors, leading to cancer, has been known for a long time.[1−5] To clarify the mechanisms of oxidative damage in these processes, numerous spectroscopic and theoretical investigations have been performed to explore the intrinsic geometric and electronic properties for isolated nucleotides, the basic building blocks of DNA molecules.[6−14] As such, a broad range of knowledge on isolated nucleotides in various charge states, that is, neutral, [dNMP], deprotonated or radical anions, $[dNMP - H]^-$/$[dNMP]^{\bullet-}$, and double-deprotonated dianions $[dNMP - 2H]^{2-}$ (N = A, G, C, or T), including their geometric and electronic structures, as well as the mechanisms of indirect and direct electron detachments, has been established.[6,7,14]

The information on isolated nucleotides is crucial to the understanding of the properties of DNA molecules. Nevertheless, their interactions with solvent water molecules remains poorly studied, despite the fact that most ionizing radiation-induced DNA damage processes take place in solution or at interfaces. Such information is especially desired since discrepancies in the properties of DNA or nucleotides in the gas phase and solutions have often been observed. However, experimental characterization of solvated biological molecules is challenging and far from settled. The challenges are related to two issues: (1) what kinds of isomers are generated and (2) how can they be spectroscopically probed; this becomes especially troublesome due to the complexity of hydration and flexibility of biological molecules. As discussed in a very recent article by Garand and co-workers,[15] the exact ensemble of isomers remains debatable and depends on how they are generated.

Infrared (IR) spectroscopy is a powerful experimental method to probe gas-phase ion molecular structure and has been widely applied. Limitations in this methodology arise, however, with increasing molecular complexity as the number of possible structures increases and the vibrational spectra become more complicated.[15] Photoelectron spectroscopy (PES) provides another spectroscopic tool to investigate gas-phase ion molecular structures and can directly probe electronic stabilization upon solvation. The obtained vertical and adiabatic detachment energies (VDE, ADE) are sensitive to the local solvation environment. Additionally PES often exhibits salient new spectral features when a charged chromophore changes upon solvation (for example, upon proton transfer, see ref 35).

It is worth emphasizing that strand breaks of DNA have been proven to occur more often in hydrated DNA than in dry DNA.[16] Moreover, the studies on nucleotide electron attachment in aqueous solutions have demonstrated different mechanisms from that in the gas phase.[17−22] The influence of proton transfer involving water molecules seems to be

Received: February 20, 2022
Accepted: March 29, 2022
Published: April 5, 2022

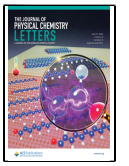

especially interesting. That process is impossible for the isolated nucleotides but may occur in water clusters or in bulk water. As indicated by the ab initio molecular dynamics (AIMD) simulations of Kohanoff et al.,[21] the protonation of anionic nucleotides in water hinders the O−P bond cleavage (a model of single strand break in DNA), which suggests that native DNA is not sensitive to hydrated electrons. The electron-attached nucleotides are well-known to be exotic,[23,24] while neutral nucleotides are generally considered protonated and deprotonated in an aqueous solution.

An effective approach to study the underlying mechanism of solvation is to investigate microsolvated clusters so that the effects from interactions between the nucleotides and each of the water molecules can be studied stepwise. For nucleotides, with a nucleobase and a phosphate group, both of which could interact with the H_2O molecule, the question of which site will preferentially bind to water molecules could be naturally raised. To date, the microsolvated clusters of nucleotides have only been studied via mass spectrometry based kinetic methods and theoretical calculations for singly protonated and deprotonated nucleotides,[25] while no spectroscopic measurements have been carried out for gaseous microsolvated nucleotide clusters to confirm conformer structures yet. Moreover, doubly deprotonated 2′-deoxynucleoside 5′-monophosphate dianions, which possesses two charged sites to bind to the H_2O molecule, were recently found to be stable in the gas phase and bring further challenges toward the analysis of binding with H_2O molecules.[14]

Figure 1 exhibits the 20 K negative ion photoelectron (NIPE) spectra of $[dGMP - 2H]^{2-}\cdot nH_2O$ (n = 1−4) (red) recorded at 157 nm (7.866 eV) and the comparison to previously recorded $[dGMP - 2H]^{2-}$ (blue[14]) spectrum (for experimental details see section 1.1 of the Supporting Information). The spectra of microsolvated clusters possess similar patterns to that of the $[dGMP - 2H]^{2-}$ anion,[14] which are composed of a distinct low-intensity band followed by a series of more intense highly congested bands. These bands represent the transitions arising from the ground electronic state of a dianion at a specific low-lying isomer to the ground and multiple electronic excited states of the corresponding singly charged anion, while the experimental ADE and VDE values are determined from the threshold and maximum of the lowest EBE (electron binding energy) band, respectively. Due to the similarities in spectral profile, we mainly focus on this band for each of the spectra of solvated clusters that reflects the ADE and VDE shift. The hydrated clusters exhibit a stepwise blue shift in EBE with increasing number of water molecules due to solvent stabilizations. The incremental ADE or VDE shifts, that is, ADE(n)/VDE(n) − ADE(n − 1)/VDE(n − 1), were measured to be 0.50, 0.25, 0.15, and 0.10 eV for n = 1, 2, 3, and 4, respectively. The first water molecule results in the strongest stabilization of 0.50 eV, 2 times bigger than that from the second water and 5 times greater compared to the effect of the fourth water molecule.

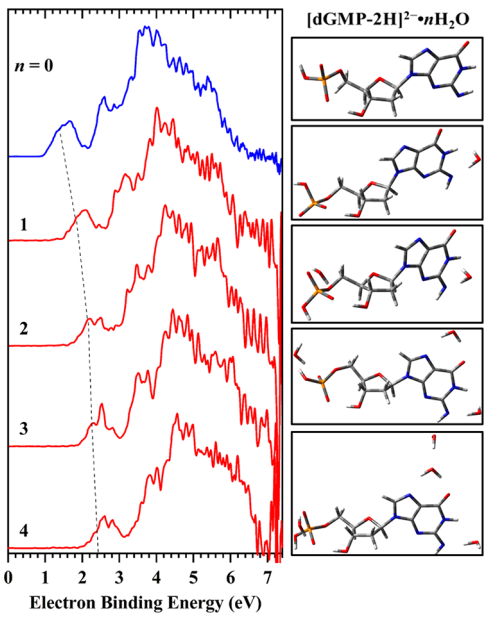

Figure 1. The 20 K NIPE spectra of $[dGMP - 2H]^{2-}\cdot nH_2O$ (n = 1−4) (red) and $[dGMP - 2H]^{2-}$ (blue, ref 14) at 157 nm (7.866 eV) (left panel) and the most stable conformations of particular clusters having VDE and ADE characteristics that reproduce the measured values (right panel). The dashed line serves as an eye-guide for the increasing trend of the VDEs as the number of water molecules increases from 0 to 4.

In order to explain the above-mentioned effects at the molecular level, we conducted conformational analysis of the microsolvated $[dGMP - 2H]^{2-}$ anion followed by VDE/ADE calculations for each identified cluster.

Various approaches were used to computationally describe microsolvation effects as this is not a trivial task. Indeed, the search for low energy conformers is an NP-hard (non-deterministic polynomial time hard) problem,[26] which generally cannot be solved by a brute-force method. An exemplary illustration of this difficulty is a recent work from Boldyrev's group,[27] who showed that for a modest discretization of spatial and angular conformational degrees of freedom, the number of initial geometries for a relatively small $NO_3^-(H_2O)_{12}$ hydrate amounts to 10^{42} initial configurations. Thus, chemical intuition,[28] water density distribution around large fragments of biological importance (e.g., around DNA),[29] molecular dynamics,[30] hybrid QM/MM approach,[31] etc., have been used in the past to solve the conformational problem in a finite time. Here, we propose another general-purpose computational approach, which is a combination of molecular dynamics simulations followed by clustering of similar configurations and their quantum chemical refinement (for computational details, see sections 1.2.1 and 1.2.2 of the Supporting Information). Our novel approach, employing clustering of similar configurations in an ensemble generated by MD simulations, seems to be relatively simple and efficient. Moreover, it results in averaged VDEs and ADEs calculated for individual low energy geometries remaining in good agreement with the experimental values as is demonstrated below.

According to our previous studies, guanosine phosphate deprotonates at the guanine amine and phosphate group, producing dianionic $[dGMP - 2H]^{2-}$ system, where negative charges are maximally separated, that is, they are localized on the phosphate group and on the purine moiety (see Scheme 1).[14] Therefore, it could be expected that polar water molecules attach to $[dGMP - 2H]^{2-}$, either close to the deprotonated phosphate group or close to the purine ring, interacting with the deprotonated N10 nitrogen. Indeed, we can observe such localization of water molecules in all the optimized $[dGMP - 2H]^{2-}\cdot H_2O$ geometries (see Figure 2). In the dominant conformation, structure one-m23 (with the highest population of 0.71; for details of how the contribution

https://doi.org/10.1021/acs.jpclett.2c00512
J. Phys. Chem. Lett. 2022, 13, 3230−3236

Scheme 1. Chemical Formula of $[dGMP - 2H]^{2-}$ along with Atom Numbering

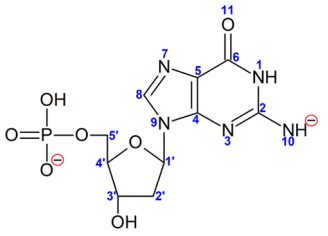

of particular geometries to the equilibrated mixture of conformers was calculated see ref 32 or section 1.2.3 of the Supporting Information) in the ensemble of conformers equilibrated at 298 K (in the following we will denote the population in the ensemble as an equilibrium fraction, x_M), see Table 1, the water molecule is bound via a hydrogen bond to the anionic deprotonated purine amine group (see Figure 2, the framed geometry). The remaining significant structures ($x_M \geq 0.01$) differ either by water localization or by phosphate group and sugar ring conformation. VDE calculated for the dominant structure amounts to 1.70 eV (for VDE and ADE definitions, see section 1.2.4 of the Supporting Information), which is in good agreement with the experimental VDE of 1.80 eV (see Table 1). The weighted average VDE_{avg}, calculated for the complete set of optimized structures, is slightly lower than VDE for the dominant structure and amounts to 1.66 eV, which additionally highlights the role of the one-m23 type of geometry in the formation of the experimental PES spectrum.

Comparing the results obtained for singly and doubly hydrated $[dGMP - 2H]^{2-}$ systems, one can state that the first water molecule localizes the most willingly near the deprotonated amine group while the second one localizes near the deprotonated phosphate group (cf. the dominant two-m19 and two-m23 structure, see Figure 3). Much less populated are geometries where both waters localize near the purine nucleobase (as in case of two-m3 or two-m24 structures, see Figure 3 and Table 2). The two almost identically stable geometries: two-m19 and two-m23, differing only slightly in the near-phosphate second water location

Table 1. Relative Gibbs Free Energy Values (ΔG, in kcal/mol) and Vertical and Adiabatic Detachment Energy (VDE and ADE, in eV), Calculated for the $[dGMP - 2H]^{2-}\cdot H_2O$ Systems at the CAM-B3LYP/6-31++G(d,p) Level, Characterized by Equilibrium Fraction $x_M \geq 0.01$[a]

name	ΔG	VDE	ADE	x_M
manual-9	2.5	1.63	1.20	0.01
one-m1	2.2	1.59	1.31	0.02
one-m2	1.6	1.64	1.33	0.05
one-m5	2.6	1.65	1.36	0.01
one-m7	2.0	1.65	1.33	0.02
one-m9	2.0	1.36	1.18	0.03
one-m12	2.6	1.59	1.31	0.01
one-m14	1.9	1.36	0.97	0.03
one-m17	1.6	1.67	1.35	0.05
one-m18	2.6	1.65	1.36	0.01
one-m20	2.0	1.70	1.38	0.03
one-m23	**0.0**	**1.70**	**1.37**	**0.71**
one-m29	2.3	1.33	0.97	0.02
weighted average		**1.66**	**1.34**	
experimental values		1.80	1.55	

[a]Data for the dominant one-m23 geometry, as well as weighted average VDE and ADE, are bolded. Characteristics for all the obtained geometries for singly hydrated $[dGMP - 2H]^{2-}$ are gathered in Table S1 in the Supplementary Information.

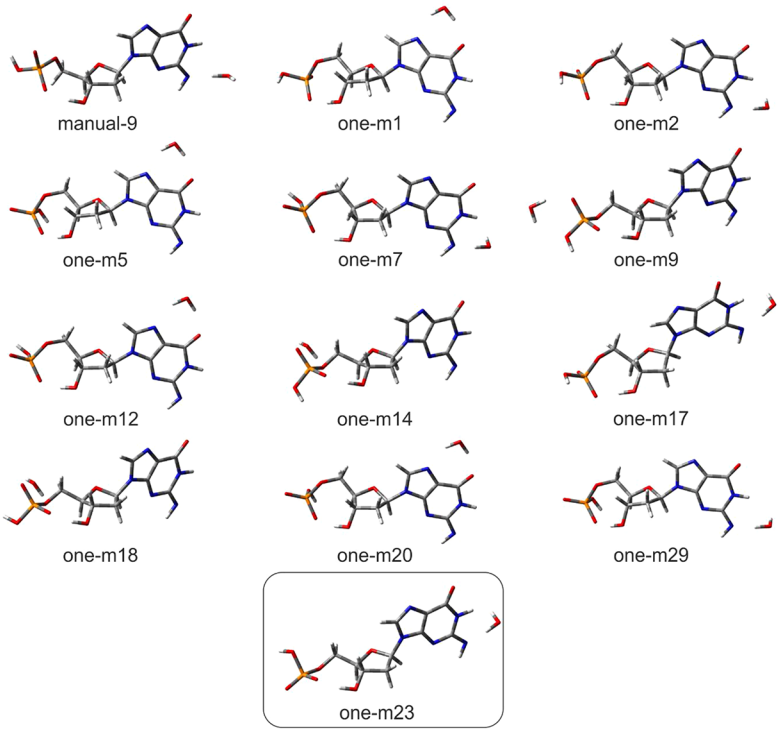

Figure 2. Visualization of dianionic singly hydrated $[dGMP - 2H]^{2-}\cdot H_2O$ structures for which equilibrium fraction amounts to $x_M \geq 0.01$, optimized at CAM-B3LYP/6-31++G(d,p) level,[33,34] along with their labels. The most stable geometry is shown in the box.

https://doi.org/10.1021/acs.jpclett.2c00512
J. Phys. Chem. Lett. 2022, 13, 3230−3236

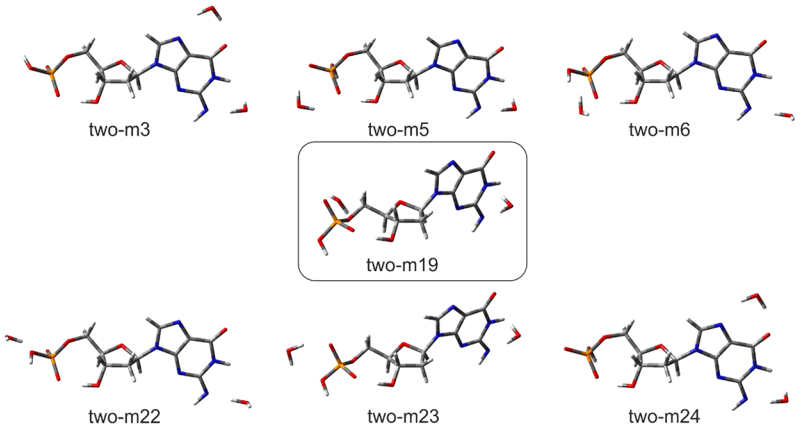

Figure 3. Visualization of dianionic doubly hydrated $[dGMP - 2H]^{2-}\cdot 2H_2O$ structures for which equilibrium fraction amounts to $x_M \geq 0.01$, optimized at CAM-B3LYP/6-31++G(d,p) level,[33,34] along with their names. The most stable geometry is shown in the box.

Table 2. Relative Gibbs Free Energy Values (ΔG, in kcal/mol) and Vertical and Adiabatic Detachment Energy (VDE and ADE, in eV), Calculated for the $[dGMP - 2H]^{2-}\cdot 2H_2O$ Systems at the CAM-B3LYP/6-31++G(d,p) Level, Characterized by Equilibrium Fraction $x_M \geq 0.01$[a]

name	ΔG	VDE	ADE	x_M
two-m3	1.4	2.00	1.62	0.04
two-m5	1.9	1.81	1.46	0.02
two-m6	2.0	1.74	1.42	0.01
two-m19	**0.0**	**1.81**	**1.32**	**0.46**
two-m22	2.1	1.75	1.42	0.01
two-m23	**0.1**	**1.81**	**1.53**	**0.39**
two-m24	1.7	2.07	1.68	0.03
weighted average		**1.82**	**1.43**	
experimental values		2.05	1.80	

[a]Data for the dominant two-19 and two-23 geometries, as well as weighted average VDE and ADE, are bolded. Characteristics for all the obtained geometries for doubly hydrated $[dGMP - 2H]^{2-}$ are gathered in Table S2 in the Supplementary Information.

possess the same VDE values (1.81 eV, comparing to 2.05 eV experimental value). As those structures dominate the doubly hydrated dianion ensemble, with the cumulative contribution of 85% (see Table 2), VDE_{avg} estimated for the doubly hydrated system is almost the same as VDE calculated for two-m19 and two-m23, hence underestimated in comparison to the experimental 2.05 eV value. Analyzing the VDEs of the conformers with $x_M \geq 0.01$, one can see that the VDE of two-m24 is similar to the experimental one (Table 2). This two-m24 structure has a different solvation pattern, as the second water molecule localizes near the purine instead of the phosphate group (see Figure 3), which may suggest that in the PES experiment also structures similar to two-m24 are populated.

When the third water molecule is taken into account, we can clearly state that the three most favorable locations for water molecules are as follows: near the amine deprotonated group, near the purine ring, and near the phosphate group (see Figure 4, for example, dominant three-m15 structure). The geometries of all the important structures differ only slightly, mostly in the phosphate group moiety and in the orientation of the near-amine-group water molecule. The only structure that is clearly different from the remaining conformations is three-m21 for which the third water forms a hydrogen bond with the near-amine-group water rather than with the guanosine anion (see Figure 4). However, this structure is rather poorly populated, with $x_M = 0.02$ (see Table 3). The calculated VDEs are in very good agreement with the experimental data. Indeed, VDE calculated for the dominant three-m15 structure amounts

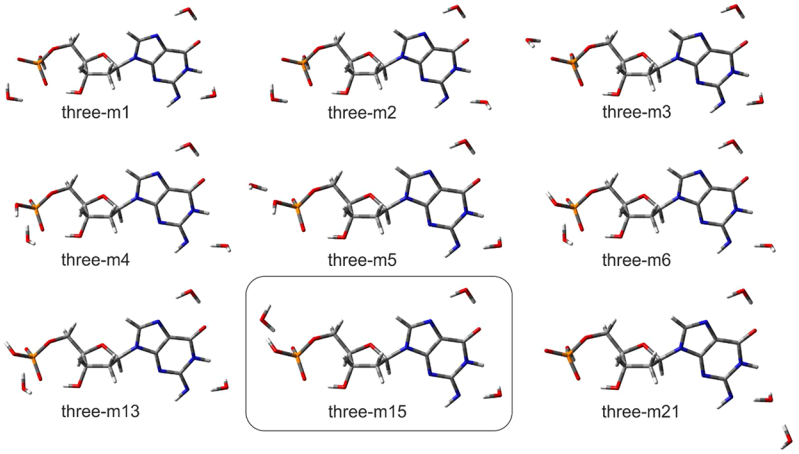

Figure 4. Visualization of dianionic triply hydrated $[dGMP - 2H]^{2-}\cdot 3H_2O$ structures, for which equilibrium fraction amounts to $x_M \geq 0.01$, optimized at CAM-B3LYP/6-31++G(d,p) level,[33,34] along with their names. The most stable geometry is shown in the box.

https://doi.org/10.1021/acs.jpclett.2c00512
J. Phys. Chem. Lett. 2022, 13, 3230−3236

Table 3. Relative Gibbs Free Energy Values (ΔG, in kcal/mol) and Vertical and Adiabatic Detachment Energy (VDE and ADE, in eV), Calculated for the $[dGMP - 2H]^{2-}\cdot 3H_2O$ Systems at the CAM-B3LYP/6-31++G(d,p) Level, Characterized by Equilibrium Fraction $x_M \geq 0.01$[a]

name	ΔG	VDE	ADE	x_M
three-m1	0.2	2.17	1.76	0.13
three-m2	0.2	2.17	1.76	0.13
three-m3	0.5	2.17	1.77	0.08
three-m4	0.2	2.09	1.72	0.12
three-m5	0.2	2.11	1.72	0.12
three-m6	0.4	2.08	1.71	0.09
three-m13	0.3	2.08	1.71	0.11
three-m15	**0.0**	**2.07**	**1.69**	**0.18**
three-m21	1.4	2.37	1.93	0.02
weighted average		**2.11**	**1.73**	
experimental values		2.20	1.95	

[a]Data for the dominant three-m15 geometry, as well as weighted average VDE and ADE, are bolded. Characteristics for all the obtained geometries for triply hydrated $[dGMP - 2H]^{2-}$ are gathered in Table S3 in the Supplementary Information.

to 2.07 eV, weighted average VDE_{avg} is equal to 2.11 eV, while the experimental value was measured at 2.20 eV.

The analysis of geometries of hydrated guanosine phosphate dianion solvated with four water molecules demonstrates that the three most favorable water locations are the same as those for the triply hydrated complex. These are near the amine group location, near the purine ring location, and near the phosphate group location. The location of the fourth water molecule is not obvious. In fact, it can localize near the phosphate group (see Figure 5, structures four-m1, -m3, -m4, -m5, -m8, -m14, -m15, and -m16) or form hydrogen bonds involving the phosphate group and ribose ring via its C3′-hydroxyl group (see four-m27 structure, Figure 5). The fourth water molecule also makes hydrogen bonds with the other water molecules, not with the guanosine phosphate dianion itself. Such a situation can be observed for the dominant four-m23 structure, where the fourth water binds to the water interacting with the purine ring (see Figure 5). One can also note that solvation by three or more water molecules leads to the stabilization of the 2′-deoxyribose conformation. Indeed, we did not observe any sugar ring conformational changes, as was noted in singly and doubly hydrated systems.

Although the system with four water molecules is the most complex, its computational characteristics are in the best agreement with the experimental ones. In fact, the VDE value for the thermodynamically most stable four-m23 system was calculated to be 2.34 eV (average VDE_{avg} is equal to 2.28 eV), while the experimental VDE for quadruply hydrated guanosine dianion was estimated at 2.30 eV (see Table 4).

Table 4. Relative Gibbs Free Energy Values (ΔG, in kcal/mol) and Vertical and Adiabatic Detachment Energy (VDE and ADE, in eV), Calculated for the $[dGMP - 2H]^{2-}\cdot 4H_2O$ Systems at the CAM-B3LYP/6-31++G(d,p) Level, Characterized by Equilibrium Fraction $x_M \geq 0.01$[a]

name	ΔG	VDE	ADE	x_M
four-m1	1.6	2.23	1.76	0.03
four-m3	2.0	2.13	1.75	0.01
four-m4	1.1	2.14	1.76	0.06
four-m5	1.7	2.14	1.76	0.02
four-m8	1.6	2.18	1.79	0.03
four-m13	0.7	2.39	1.97	0.12
four-m14	1.1	2.17	1.79	0.06
four-m15	1.1	2.25	1.84	0.06
four-m16	0.8	2.12	1.75	0.10
four-m23	**0.0**	**2.34**	**1.90**	**0.38**
four-m27	1.7	2.24	1.82	0.02
four-m31	0.8	2.37	1.97	0.10
weighted average		**2.28**	**1.73**	
experimental values		2.30	2.05	

[a]Data for the dominant four-m23 geometry, as well as weighted average VDE and ADE, are bolded. Characteristics for all the obtained geometries for quadruply hydrated $[dGMP - 2H]^{2-}$ are gathered in Table S4 in the Supplementary Information.

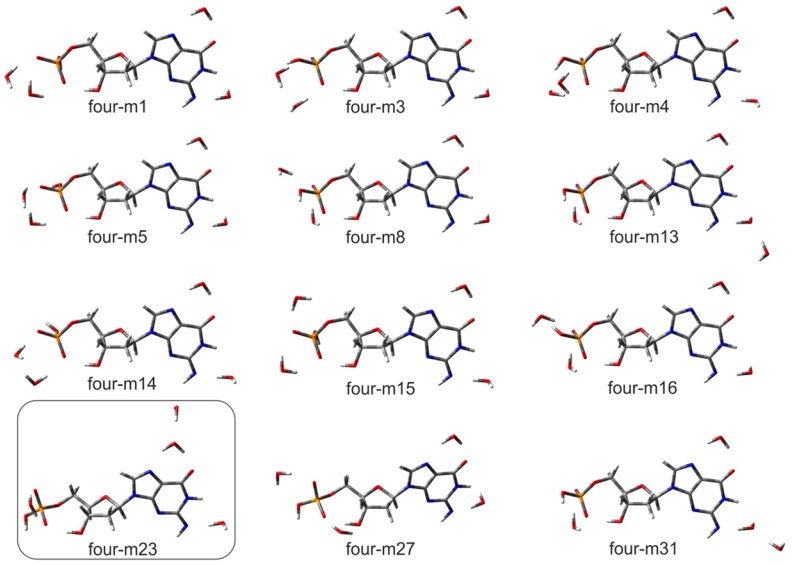

Figure 5. Visualization of dianionic $[dGMP - 2H]^{2-}\cdot 4H_2O$ structures, hydrated with four water molecules, for which equilibrium fraction amounts to $x_M \geq 0.01$, optimized at CAM-B3LYP/6-31++G(d,p) level,[33,34] along with their names. The most stable geometry is shown in the box.

https://doi.org/10.1021/acs.jpclett.2c00512
J. Phys. Chem. Lett. 2022, 13, 3230−3236

In summary, we proposed a general-purpose computational method to study microsolvated systems. Our approach is based on a series of MD calculations followed by clustering of similar structures. This leads to a set of geometries, which are then subjected to quantum chemical calculations enabling the experimental characteristics (such as ADE and VDE) to be predicted. We used this approach, MD/clustering/QM, to study microsolvation for the dianion of doubly deprotonated 5′-monophosphate of guanosine, a system that was recently found to be stable in the gas phase. The water clusters, $[dGMP - 2H]^{2-}\cdot nH_2O$ (n = 1−4), were measured with NIPE spectroscopy, and we demonstrated that the computational characteristics obtained by our MD/clustering/QM methodology are in pretty good accordance with the experimental values. As a consequence, for the first time our studies provided a "molecular structure" of the ensembles of gaseous microsolvated nucleotide clusters.

The strength of hydrogen bonds determines the specific water coordination sites in the studied clusters. Therefore, in the lowest energy configurations of the singly and doubly hydrated anion, water molecules form very strong hydrogen bonds with two charged moieties: the deprotonated amine and the phosphate group. The third water molecule in the triply hydrated anion preferentially occupies an energetically favorable site that allows it to make two hydrogen bonds with the N10 and O11 sites (for numbering, see Scheme 1). Furthermore, for the quadruply hydrated anion, the fourth water molecule interacts with the water already bonded to the guanine moiety (Figure 5, four-m23), which suggests that polarization of the bonded molecule due to hydrogen bonding with the guanine moiety makes it favorably interact with other waters or activates it for interaction with other waters. Note a similar pattern present in other low energy conformations of the quadruply hydrated anion (e.g., see four-m13 and four-m31 in Figure 5).

Water binding energies (WBEs), in terms of the free energy of cluster formation ($\Delta G_{hydr\text{-}BSSE}$ − difference between the free energy of cluster and the sum of the free energies of isolated monomers corrected for basis set superposition error (BSSE); see section 1.2.5 in the Supporting Information for details on the calculation of WBE), are equal to −18.0, −22.9, −26.7, and −30.5 kcal/mol for $[dGMP - 2H]^{2-}\cdot H_2O$, $[dGMP - 2H]^{2-}\cdot 2H_2O$, $[dGMP - 2H]^{2-}\cdot 3H_2O$, and $[dGMP - 2H]^{2-}\cdot 4H_2O$, respectively (see Table S5 in the Supporting Information). Interestingly, the WBE per water molecule, $\Delta G_{hydr\text{-}BSSE}/n$ (where n stands for the number of water molecules in a given cluster), is perfectly linearly correlated (R^2 = 1.000) with the increase of VDE with the number of water molecules (see Figure S1 in the Supporting Information). For the most stable cluster of the quadruply hydrated dianion, one of the water molecules makes hydrogen bonds with another water rather than with the nucleotide moiety, which suggests that further increase in the number of waters may facilitate proton transfer (PT) from a water interacting directly with the nucleotide. Indeed, a product of such a PT process, the hydroxyl anion, can be stabilized by additional waters.[35] Thus the proposed approach opens a route to the systematic studies of hydration effects in transition from the gas phase to bulk water. It is difficult to overestimate the importance of this issue in the DNA context, since interactions between a solute and water may qualitatively change the chemistry triggered by electron attachment in DNA based systems. The approach presented in the current work might, thus, lead to understanding of the very different sensitivity of native DNA to electrons in vacuum and under physiological conditions.

■ ASSOCIATED CONTENT

Supporting Information

The Supporting Information is available free of charge at https://pubs.acs.org/doi/10.1021/acs.jpclett.2c00512.

Experimental methods and computational details along with the corresponding references, relative Gibbs free energy values, VDE, ADE and equilibrium ratio (x_M) values calculated at CAM-B3LYP/6-31++G(d,p) level, for the obtained $[dGMP - 2H]^{2-}\cdot nH_2O$ systems (n = 1−4), water binding energies, plot of water binding energy per water molecule vs experimental VDE increment (PDF)

■ AUTHOR INFORMATION

Corresponding Authors

Xue-Bin Wang − *Physical Sciences Division, Pacific Northwest National Laboratory, Richland, Washington 99352, United States;* orcid.org/0000-0001-8326-1780; Email: xuebin.wang@pnnl.gov

Janusz Rak − *Faculty of Chemistry, University of Gdańsk, Gdańsk 80-308, Poland;* orcid.org/0000-0003-3036-0536; Email: janusz.rak@ug.edu.pl

Authors

Samanta Makurat − *Faculty of Chemistry, University of Gdańsk, Gdańsk 80-308, Poland;* orcid.org/0000-0003-2907-7725

Qinqin Yuan − *Physical Sciences Division, Pacific Northwest National Laboratory, Richland, Washington 99352, United States; Department of Chemistry, Anhui University, Hefei, Anhui 230601, China*

Jacek Czub − *Department of Physical Chemistry and BioTechMed Center, Gdańsk University of Technology, Gdańsk 80-233, Poland;* orcid.org/0000-0003-3639-6935

Lidia Chomicz-Mańka − *Faculty of Chemistry, University of Gdańsk, Gdańsk 80-308, Poland*

Wenjin Cao − *Physical Sciences Division, Pacific Northwest National Laboratory, Richland, Washington 99352, United States;* orcid.org/0000-0002-2852-4047

Complete contact information is available at: https://pubs.acs.org/10.1021/acs.jpclett.2c00512

Author Contributions

#S.M., Q.Y., J.C., and L.C.-M. contributed equally to this work.

Notes

The authors declare no competing financial interest.

The Molecular Dynamics input and output files, as well as the Gaussian output files containing CAM-B3LYP data of optimized dianions and their corresponding anion radicals will be deposited to the zenodo.org repository, DOI: 10.5281/zenodo.5808759, upon publication.

■ ACKNOWLEDGMENTS

This work was supported by Polish National Science Center (NCN) under the CEUS-UNISONO Grant No. UMO-2020/02/Y/ST4/00110. Computations were performed with PLGrid Infrastructure (plgsamanta) and the Wroclaw Center for Networking and Supercomputing (wcss.wroc.pl, grant

209). The PES work was supported by U.S. Department of Energy (DOE), Office of Basic Energy Sciences, Division of Chemical Science, Geosciences, and Biosciences, and performed using EMSL, a national scientific user facility sponsored by DOE's Office of Biological and Environmental Research and located at Pacific Northwest National Laboratory, which is operated by Battelle Memorial Institute for the DOE.

REFERENCES

(1) Schulte-Frohlinde, D.; Simic, M.; Görner, H. Laser-induced Strand Break Formation in DNA and Polynucleotides. *Photochem. Photobiol.* **1990**, *52*, 1137−1151.
(2) Görner, H.; Gurzadyan, G. G. Photolysis of Polycytidylic Acid on 193 nm Laser Excitation. *J. Photochem. Photobiol., A* **1993**, *71*, 155−160.
(3) Melvin, T.; Botchway, S.; Parker, A.; O'Neill, P. Induction of Strand Breaks in Single-Stranded Polyribonucleotides and DNA by Photoionization: One Electron Oxidized Nucleobase Radicals as Precursors. *J. Am. Chem. Soc.* **1996**, *118*, 10031−10036.
(4) Hall, D. B.; Holmlin, R. E.; Barton, J. K. Oxidative DNA Damage Through Long-Range Electron Transfer. *Nature* **1996**, *382*, 731−735.
(5) Fernando, H.; Papadantonakis, G. A.; Kim, N. S.; LeBreton, P. R. Conduction-Band-Edge Ionization Thresholds of DNA Components in Aqueous Solution. *Proc. Natl. Acad. Sci. U. S. A.* **1998**, *95*, 5550−5555.
(6) Yang, X.; Wang, X.-B.; Vorpagel, E. R.; Wang, L.-S. Direct Experimental Observation of the Low Ionization Potentials of Guanine in Free Oligonucleotides by Using Photoelectron Spectroscopy. *Proc. Natl. Acad. Sci. U. S. A.* **2004**, *101*, 17588−17592.
(7) Chatterley, A. S.; Johns, A. S.; Stavros, V. G.; Verlet, J. R. R. Base-Specific Ionization of Deprotonated Nucleotides by Resonance Enhanced Two-Photon Detachment. *J. Phys. Chem. A* **2013**, *117*, 5299−5305.
(8) Zakjevskii, V. V.; King, S. J.; Dolgounitcheva, O.; Zakrzewski, V. G.; Ortiz, J. V. Base and Phosphate Electron Detachment Energies of Deoxyribonucleotide Anions. *J. Am. Chem. Soc.* **2006**, *128*, 13350−13351.
(9) Rubio, M.; Roca-Sanjuan, D.; Serrano-Andres, L.; Merchan, M. Determination of the Electron-Detachment Energies of 2 '-Deoxyguanosine 5 '-Monophosphate Anion: Influence of the Conformation. *J. Phys. Chem. B* **2009**, *113*, 2451−2457.
(10) Nei, Y.-W.; Hallowita, N.; Steill, J.; Oomens, J.; Rodgers, M. Infrared Multiple Photon Dissociation Action Spectroscopy of Deprotonated DNA Mononucleotides: Gas-Phase Conformations and Energetics. *J. Phys. Chem. A* **2013**, *117*, 1319−1335.
(11) Chatterley, A. S.; West, C. W.; Stavros, V. G.; Verlet, J. R. Time-Resolved Photoelectron Imaging of the Isolated Deprotonated Nucleotides. *Chem. Sci.* **2014**, *5*, 3963−3975.
(12) Cercola, R.; Matthews, E.; Dessent, C. E. Photoexcitation of Adenosine 5′-Triphosphate Anions in Vacuo: Probing the Influence of Charge State on the UV Photophysics of Adenine. *J. Phys. Chem. B* **2017**, *121*, 5553−5561.
(13) Castellani, M. E.; Avagliano, D.; Verlet, J. R. Ultrafast Dynamics of the Isolated Adenosine-5′-Triphosphate Dianion Probed by Time-Resolved Photoelectron Imaging. *J. Phys. Chem. A* **2021**, *125*, 3646−3652.
(14) Yuan, Q.; Chomicz-Mańka, L.; Makurat, S.; Cao, W.; Rak, J.; Wang, X.-B. Photoelectron Spectroscopy and Theoretical Investigations of Gaseous Doubly Deprotonated 2'-Deoxynucleoside 5′-Monophosphate Dianions. *J. Phys. Chem. Lett.* **2021**, *12*, 9463−9469.
(15) Sherman, S. L.; Nickson, K. A.; Garand, E. Comment on "Microhydration of Biomolecules: Revealing the Native Structures by Cold Ion IR Spectroscopy". *J. Phys. Chem. Lett.* **2022**, *13*, 2046−2050.
(16) Adhikary, A.; Becker, D.; Sevilla, M. D. Electron Spin Resonance of Radicals in Irradiated DNA. In *Applications of EPR in Radiation Research*; Springer: 2014; pp 299−352.
(17) Gu, J.; Xie, Y.; Schaefer, H. F., III Electron Attachment to Nucleotides in Aqueous Solution. *ChemPhysChem* **2006**, *7*, 1885−1887.
(18) Schyman, P.; Laaksonen, A. On the Effect of Low-Energy Electron Induced DNA Strand Break in Aqueous Solution: A Theoretical Study Indicating Guanine as a Weak Link in DNA. *J. Am. Chem. Soc.* **2008**, *130*, 12254−12255.
(19) Pluharova, E.; Jungwirth, P.; Bradforth, S. E.; Slavicek, P. Ionization of Purine Tautomers in Nucleobases, Nucleosides, and Nucleotides: from the Gas Phase to the Aqueous Environment. *J. Phys. Chem. B* **2011**, *115*, 1294−1305.
(20) Smyth, M.; Kohanoff, J. Excess Electron Interactions with Solvated DNA Nucleotides: Strand Breaks Possible at Room Temperature. *J. Am. Chem. Soc.* **2012**, *134*, 9122−9125.
(21) McAllister, M.; Smyth, M.; Gu, B.; Tribello, G. A.; Kohanoff, J. Understanding the Interaction Between Low-Energy Electrons and DNA Nucleotides in Aqueous Solution. *J. Phys. Chem. Lett.* **2015**, *6*, 3091−3097.
(22) Ma, J.; Wang, F.; Denisov, S. A.; Adhikary, A.; Mostafavi, M. Reactivity of Prehydrated Electrons Toward Nucleobases and Nucleotides in Aqueous Solution. *Sci. Adv.* **2017**, *3*, No. e1701669.
(23) Stokes, S. T.; Grubisic, A.; Li, X.; Jae Ko, Y.; Bowen, K. H. Photoelectron Spectroscopy of the Parent Anions of the Nucleotides, Adenosine-5′-monophosphate and 2′ Deoxyadenosine-5′-Monophosphate. *J. Chem. Phys.* **2008**, *128*, 044314.
(24) Kobyłecka, M.; Gu, J.; Rak, J.; Leszczynski, J. Barrier-free Proton Transfer in the Valence Anion of 2′-Deoxyadenosine-5′-monophosphate. II. A Computational Study. *J. Chem. Phys.* **2008**, *128*, 044315.
(25) Liu, D.; Wyttenbach, T.; Bowers, M. T. Hydration of Mononucleotides. *J. Am. Chem. Soc.* **2006**, *128*, 15155−15163.
(26) Deaven, D. M.; Ho, K. M. Molecular geometry optimization with a genetic algorithm. *Phys. Rev. Lett.* **1995**, *75*, 288−291.
(27) Tkachenko, N. V.; Tkachenko, A. A.; Kulyukin, V. A.; Boldyrev, A. I. DFT Study of Microsolvated $[NO_3{\cdot}(H_2O)_n]^-$ (n = 1−12) Clusters and Molecular Dynamics Simulation of Nitrate Solution. *J. Phys. Chem. A* **2021**, *125*, 8899−8906.
(28) Bao, X.; Liang, G.; Wong, N.-B.; Gu, J. Microsolvation Pattern of the Hydrated Radical Anion of Uracil: $U^-(H_2O)_n$ (n = 3−5). *J. Phys. Chem. A* **2007**, *111*, 666−672.
(29) Kumar, A.; Sevilla, M. D. Influence of Hydration on Proton Transfer in the Guanine-Cytosine Radical Cation ($G^{\bullet+}$-C) Base Pair: A Density Functional Theory Study. *J. Phys. Chem. B* **2009**, *113*, 11359−11361.
(30) Kabelac, M.; Hobza, P. At Nonzero Temperatures, Stacked Structures of Methylated Nucleic Acid Base Pairs and Microhydrated Nonmethylated Nucleic Acid Base Pairs are Favored over Planar Hydrogen-Bonded Structures: A Molecular Dynamics Simulations Study. *Chem.—Eur. J.* **2001**, *7*, 2067−2074.
(31) Jia, Y.; Xiao, H.; Li, Y. L.; Bai, Q. H.; Xue, Y.; Kim, C. K.; Gao, J. Y. Insight into Substituent Effects on the Hydrolysis of Amidines by a Microhydration Model. *Theor. Chem. Acc.* **2017**, *136*, 68.
(32) Rak, J.; Skurski, P.; Simons, J.; Gutowski, M. Low-Energy Tautomers and Conformers of Neutral and Protonated Arginine. *J. Am. Chem. Soc.* **2001**, *123*, 11695−11707.
(33) Yanai, T.; Tew, D.; Handy, N. A New Hybrid Exchange-Correlation Functional Using the Coulomb-Attenuating Method (CAM-B3LYP). *Chem. Phys. Lett.* **2004**, *393*, 51−57.
(34) Wang, F.; Hu, Z.; Wang, X. B.; Sun, Z.; Sun, H. Assessment of DFT Methods for the Prediction of Detachment Energies and Electronic Structures of Complex and Multiply Charged Anions. *Comput. Theor. Chem.* **2021**, *1202*, 113295.
(35) Li, R.-Z.; Deng, S. H.; Hou, G.-L.; Valiev, M.; Wang, X.-B. Photoelectron Spectroscopy of Solvated Dicarboxylate and Alkali Metal Ion Clusters, $M^+[O_2C(CH_2)_2CO_2]^{2-}[H_2O]_n$ (M = Na, K; n = 1−6). *Phys. Chem. Chem. Phys.* **2018**, *20*, 29051−29060.

https://doi.org/10.1021/acs.jpclett.2c00512
J. Phys. Chem. Lett. 2022, 13, 3230−3236